



HAL
open science

Geopolymer as dielectric materials for ultra-wideband antenna applications: Impact of magnetite addition and humidity

Ioana Nicoleta Vlasceanu, Amine Gharzouni, Olivier Tantot, Michèle Lalande, Catherine Elissalde, Sylvie Rossignol

► To cite this version:

Ioana Nicoleta Vlasceanu, Amine Gharzouni, Olivier Tantot, Michèle Lalande, Catherine Elissalde, et al.. Geopolymer as dielectric materials for ultra-wideband antenna applications: Impact of magnetite addition and humidity. *Open Ceramics*, 2020, 2, 100013 (9 p.). 10.1016/j.oceram.2020.100013 . hal-02956280

HAL Id: hal-02956280

<https://hal.science/hal-02956280>

Submitted on 5 Oct 2020

HAL is a multi-disciplinary open access archive for the deposit and dissemination of scientific research documents, whether they are published or not. The documents may come from teaching and research institutions in France or abroad, or from public or private research centers.

L'archive ouverte pluridisciplinaire **HAL**, est destinée au dépôt et à la diffusion de documents scientifiques de niveau recherche, publiés ou non, émanant des établissements d'enseignement et de recherche français ou étrangers, des laboratoires publics ou privés.



Geopolymer as dielectric materials for ultra-wideband antenna applications: Impact of magnetite addition and humidity



I.N. Vlasceanu^a, A. Gharzouni^a, O. Tantot^b, M. Lalande^c, C. Elissalde^d, S. Rossignol^{a,*}

^a IRCER, UMR CNRS 7315, 12 rue Atlantis, 87068, Limoges Cedex, France

^b XLIM, UMR CNRS 7252, 123 avenue Albert Thomas, 87060, Limoges Cedex, France

^c XLIM, UMR CNRS 7252, 7 rue Jules Vallès, 19100, Brive La Gaillarde, France

^d ICMCB, UMR CNRS 5026, 87 Avenue du Dr A. Schweitzer, Pessac, 33608, France

ARTICLE INFO

Keywords:

Geopolymer
Dielectric properties
Antenna
Humidity
Magnetite

ABSTRACT

Cost-efficiency, environmental sustainability, and dimension reduction are important aspects in wideband antenna design. Geopolymers could be an eco-friendly and cost-efficient solution for this application. The objective of this work is to develop new geopolymer-based composites with tailored dielectric properties for applications in radar antennas. For this, different formulations based on three metakaolin and two alkaline solutions were tested. The influence of magnetite was studied by insertion of 1, 5 or 10 wt % of Fe₃O₄ in different formulations. Furthermore, the influence of humidity was also emphasized. Dielectric investigations between 2 and 3.3 GHz were performed. The results showed that the metakaolin type had no effect on the dielectric characteristics, whereas the nature of activation alkaline solution had a significant influence. Indeed, an increase in permittivity from 3.5 to 5.9 is evidenced by the change in the alkaline solution. The addition of magnetite up to 10 wt % had a little influence on the polycondensation reaction and lead to a slight increase in permittivity and permeability values. Furthermore, the permittivity and the loss tangent increase at high relative humidity level, but the phenomenon is reversible. It was also demonstrated that time had no effect on the permittivity values.

1. Introduction

An antenna is the interface between radiofrequency (RF) waves propagating through space and electric currents moving in metal conductors, used with a transmitter or receiver (IEEE standard 145–1983) [1,2]. Nowadays, miniaturization of wideband antennas is necessary to obtain compact devices such as wearable and/or disposable ones [3], or related to the Internet of Things (IoT) [4], microwave imaging [5] and Ultra-wideband (UWB) antennas – the application topics discussed herein [6]. UWB antennas have traditional use in non-cooperative radar imaging. In terms of both civil and military use, it gained widespread attention for its implementation in synthetic aperture radar (SAR) technology. However, most recent applications target sensor data collection, precision locating and tracking applications. Unlike broad spectrum, UWB transmits in a manner that does not interfere with conventional narrowband and carrier wave transmission in the same frequency band. Reducing dimensions of the antenna affects the electrical and field properties such as radiation pattern stability, gain, and efficiency [7].

Innovative dielectric materials based on geopolymers represent a

cost-efficient and eco-friendly alternative to current materials used in electronics and electric engineering applications [7]. Geopolymers are synthesized by the reaction of an aluminosilicate (powder) with an alkaline solution [8,9]. Increasing interest has been drawn in recent years to the dielectric properties of geopolymers. It was previously shown that such geopolymer-based antennas can properly operate in a frequency band ranging from 300 MHz to 3 GHz [9]. Furthermore, it has been demonstrated that for fly ash based geopolymers the dielectric properties depend at early ages, on both the solution content and viscosity. However, at later ages, they are dependent on the porosity and the density of the geopolymer [10]. Different additives have also been added to geopolymer matrix to stabilize the properties. Essaidi et al. [11] investigated the dielectric properties of a geopolymer matrix for RF applications. They have demonstrated that various high-k dielectric materials, *i.e.* zirconia (ZrO₂), barium titanate (BaTiO₃) and yttria (Y₂O₃) and with a high percentage up to 60%, can be added to geopolymers to improve the dielectric properties. Magneto-dielectric substrates such as ferrite can also be used for antenna miniaturization [12]. Furthermore, the magnetic properties of magnetite were demonstrated to strongly depend on their

* Corresponding author.

E-mail address: sylvie.rossignol@unilim.fr (S. Rossignol).

<https://doi.org/10.1016/j.oceram.2020.100013>

Received 8 May 2020; Received in revised form 6 July 2020; Accepted 7 August 2020

Available online 22 August 2020

2666-5395/© 2020 Published by Elsevier Ltd on behalf of European Ceramic Society. This is an open access article under the CC BY-NC-ND license ([http://](http://creativecommons.org/licenses/by-nc-nd/4.0/)

creativecommons.org/licenses/by-nc-nd/4.0/).

synthesis method, particle size and surface treatment [13]. Electromagnetic properties investigations show that both the real and the imaginary parts of the permittivity greatly increase with aspect ratio (shape vs. dimension) increase, while the dielectric loss tangent is reduced [14].

Another important aspect influencing the dielectric properties of several materials is the water content and the relative humidity. For example, for ceramics materials, the influence of humidity on dielectric properties was related to the composition, the compacting pressure and the firing temperature and time [15]. The effect of humidity exposure on the electrical properties of porous zirconia ceramics have been also investigated [16]. It was demonstrated that the replacement of air by water (higher dielectric constant than air) leads to an increase of dielectric permittivity. An increase of the dielectric constant and of the loss tangent was also evidenced for composites based on nano-alumina and polyethylene [17,18] after absorption of water especially in the interface of filler/fibre and matrix [17,18]. For geopolymer materials, it has been evidenced that the dielectric constant and losses increase with the increase the free water content [19]. This is explained by the free cation transference under the influence of an electric field. The drying at a temperature of 300 °C eliminates this water and decreases the dielectric loss. The use of acid based geopolymer permits also to decrease the dielectric loss down to 10^{-3} because the ion transfer becomes negligible [19].

Despite many investigations, there is still a lack of information in literature concerning, on one hand, the effect of magnetite on the dielectric properties and the polycondensation reaction of geopolymers, and on the other hand, on the effect of humidity on the dielectric properties of geopolymers that is still not obvious. The objective of this work is to develop new geopolymer compositions with tailored dielectric properties for applications in radar. The influence of magnetite is studied, and the influence of humidity is also emphasized with respect to the tested compositions and formulations. Finally, dielectric investigations between 2 and 3.3 GHz have been performed, validating the functionality of the antenna devices.

2. Materials and methods

2.1. Materials and synthesis

The materials used for the synthesis of the produced geopolymer samples were: two types of silicate solution Sa and Sb with Si/K molar ratios of 0.54 and 0.67, respectively and three types of metakaolin Ma, Mb, Mc with different Si/Al molar ratio 1.17, 1 and 1.44 [22], respectively. In order to obtain a material with dielectric properties 1, 5 or 10 wt % of Fe₃O₄ (Alfa Aesar, particle size 44 μm, and 97% purity) were used. Fig. 1A shows the synthesis protocol of geopolymer samples. The silicate solution was combined with the metakaolin and with different quantities of magnetite. The obtained mixtures were placed in a closed plastic mold at 70 °C for 1 day. Next, they were dried at 90 °C for 1 day. Samples for dielectric measurements were made as it is presented in Fig. 1B. The metallic mold is fixed using screws and screw nuts on the polyethylene plate. The reactive mixture is casted in the metallic mold and covered. Samples are kept at 70 °C for 1 day and after is removed from the plates and dried in vertical position for 1 day. After drying process, the samples presented no cracks for some compositions (Fig. 1Ba) or presented some cracks around the corners (Fig. 1Bb). The cracks can be explained by the different coefficients of thermal expansion of geopolymers detailed in results. In order to investigate the influence of humidity, samples were kept in controlled humidity. The cycle of humidity treatment is presented in Fig. 2. During the first 12 days, samples were kept at 20 °C at 50% humidity and then at 85% humidity for 5 days, then the humidity was changed back to 50% for 3 more days. Nomenclature and composition (Si/Al and Si/K molar ratios) of samples is presented in Table 1. Samples are identified as SxMyF_z, where S represents the type of solution used (Sa or Sb), M the type of metakaolin (Ma, Mb or Mc), F the percentage of magnetite used (1, 5 or 10%) in the

composition.

2.2. Technical characterization

Fourier transform infrared (FTIR) spectroscopies were obtained on a fresh geopolymer paste using a Thermo Fisher Scientific Nicolet 380 using the mode attenuated total reflectance (ATR). A few drops of the reactive mixture are simply deposited on the diamond before scanning. The scans are made every 10 min for 12 h and are performed between 500 and 4000 cm⁻¹, the number of scans is 72 and the resolution is 4 cm⁻¹. The data were than treated using OMNIC program. The CO₂ in the air produce perturbations on the signal between 2400 and 2280, straight line was used on that part of the spectra in order to eliminate the noise. An automatic correction of the base line and normalization of the spectra were also done in order to compare different results. The evolution of Si–O–M (M = Si, Al) peak position over time is then plotted and the shift value (initial peak position at 0 min (directly after mixing of the precursors) –final peak position at 720 min (after consolidation) is determined. According to previous work [20], the shift value indicates the substitution of Si–O–Si bond by Si–O–Al bonds revealing the polycondensation reaction and the formed network.

Thermogravimetric analysis (TGA) and differential thermal gravimetry (DTG) were performed with an SDT Q600 equipment from TA Instruments. A heating rate of 5 °C/min was employed between 25 and 800 °C followed by a dwell of 15 min at 800 °C, in synthetic air flow (100 sccm). A platinum crucible was used. Samples kept at room temperature and in humidity (HR 85%, 20 °C) for 3 days were analyzed with this technique. TGA-DTG analysis were performed on grinded geopolymers.

Dielectric measurements were carried out by using the Network Analyzer Keysight E5063A which provided high-precision scattering parameter measurements (related to the reflection and transmission coefficients at material interfaces and through the material of a microwave electromagnetic field). For a lower influence of surface and heterogeneity defects and to obtain more homogeneous measurements and characterization of the samples, the loaded rectangular waveguide method was chosen despite its reduced frequency band in mono mode operation ($f_{c_{TE10}} = 1.735$ GHz and $f_{c_{TE20}} = 3.47$ GHz for WR340 standard of this study) Fig. 3. To duplicate the means of multi-site characterization and ensure a good level of adaptation, it was decided to carry out the transitions from the coaxial guide to the rectangular one. The guiding idea in the design is to facilitate the casting of geopolymers in the sample holder and improve its performance in terms of adaptation of the order of 25 dB between 2 and 3.3 GHz. TRL calibration of the Network Analyser gives results in a measurement error better than of |S_{ij}| 0.03 dB and arg(S_{ij}) 0.4°. Measurements of standard samples (plexiglass and Teflon) were made and comparisons of complex permittivity extracted by NRW algorithm [21,22] and by another free space method [23] have shown good agreements and validated the whole process. The sample is connected by a phase and amplitude stable cable to a VNA which is then calibrated with standards thru, reflect and line for WR340. Fig. 4 shows an example of dielectric measurements of SbMa samples 2 and 3.3 GHz. Dielectric measurements were investigated the values of the real part of dielectric constant known as the relative dielectric constant (ϵ'_r) (please see the appendices) which indicates the ability of the material to store microwave energy and tan δ , dielectric losses quantifies a dielectric material's inherent dissipation of electromagnetic energy. The values of ϵ for frequencies between 2 and 3.3 GHz for this composition were around 3.5, while tan δ values were around 0.025.

3. Results and discussions

3.1. Feasibility of the various samples

Table 2 presents the visual aspect of the samples based on Sb solution with two types of metakaolin (Ma and Mc) containing different percentage of magnetite (1, 5 or 10%). Samples made with metakaolin Ma

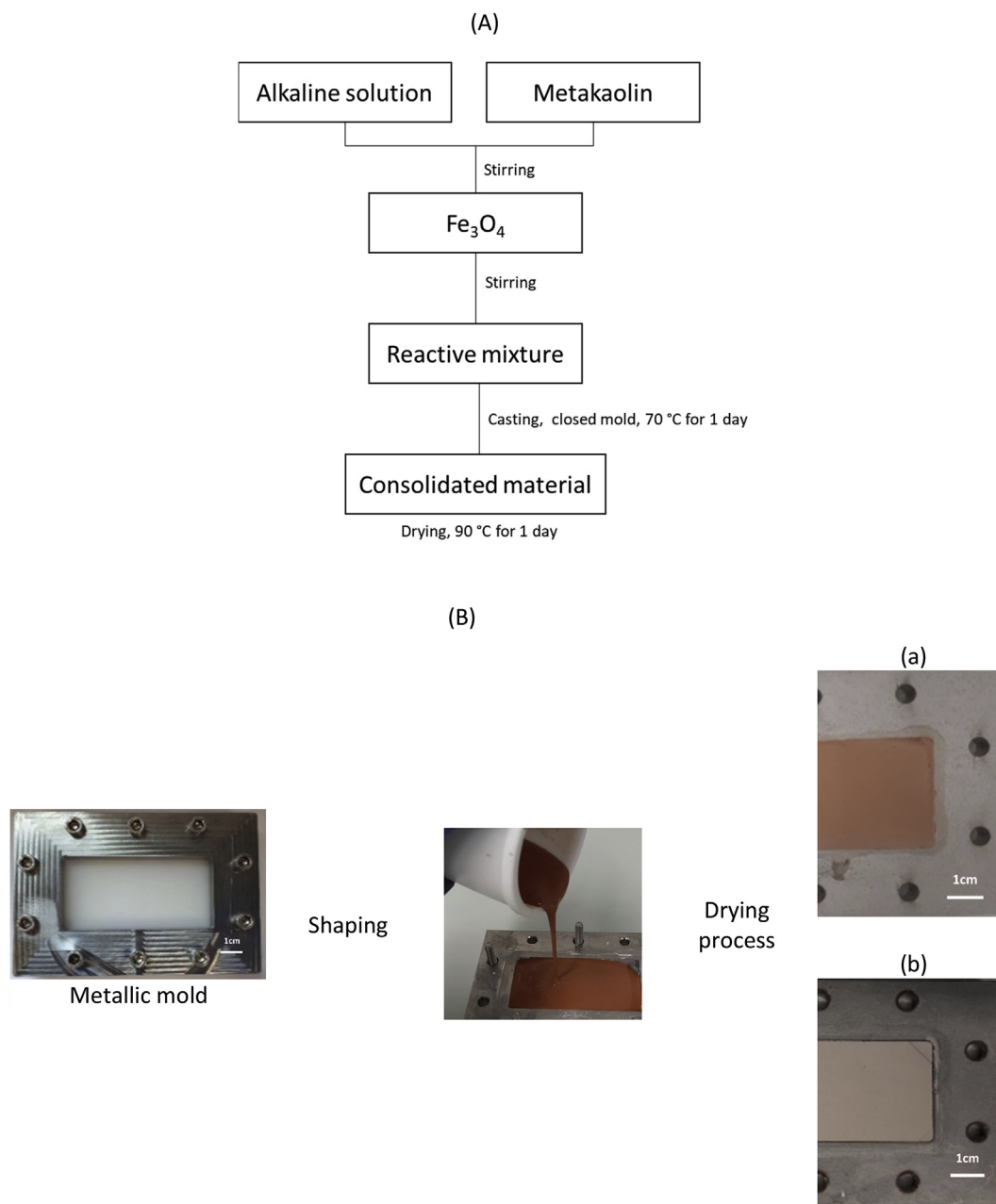


Fig. 1. (A) Synthesis protocol of geopolymers samples and (B) shaping for dielectric measurements for samples (a) without cracks and (b) with cracks after drying process figure.

without magnetite present a grey-yellow color due to the Ma initial color and purity ($\text{Si}/\text{Al} = 1.17$) [24]. The sample made with Mc presents a red-brown color caused by the presence of Fe_2O_3 [22]. Addition of 1, 5 and 10% of magnetite to samples made with metakaolin Ma induces a dark grey color due to black color of the magnetite [25]. The sample made with Mc presented a lighter grey color, compared with Ma based samples, caused by the red-brown initial color of the metakaolin. Samples made with metakaolin Ma presented cracks after drying process, while Mc based samples presented no cracks due to a higher content of impurities. These impurities play the role of filler and reinforce the microstructure [26].

3.2. Impact of magnetite addition

3.2.1. Structural data

Compositions based on Sb solution with different type of metakaolin

(Ma and Mc) with or without magnetite addition were investigated by FTIR spectroscopy (Fig. 5). Fig. 5a presents an example of three infrared spectra recorded at 0, 360 and 720 min for SbMa sample.

All the spectra show contributions located at 3255 and 1620 cm^{-1} and attributed to the ν_{OH} and δ_{OH} respectively [27]. The band observed at 980 cm^{-1} is related to Si-O-M ($M = \text{Si}$ or Al) bond. It is worth noting that the intensity of the ν_{OH} and δ_{OH} bands decreases and the Si-O-M peak position shifts towards lower wavenumber in function of time. This result is in accordance with the previous work and evidences the polycondensation reaction [28]. Fig. 5b shows the Si-O-M peak position versus time for samples based on Sb solution and Ma and Mc metakaolin without magnetite insertion and with 5% of magnetite addition. For all compositions, the initial band positions are at around 976 cm^{-1} are similar. Indeed, at $t = 0$ min, immediately upon mixing the precursors, the initial band position is imposed by the used alkaline solution and corresponds to the vibration of silicate species (the same alkaline solution

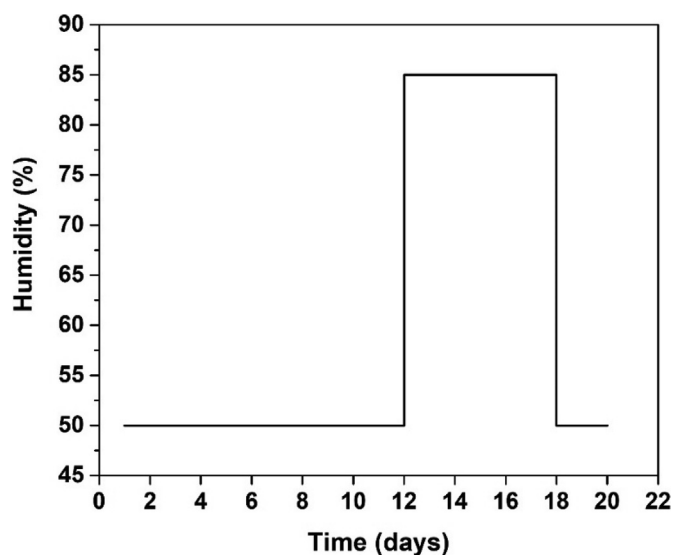


Fig. 2. Example of humidity cycle used for dielectric measurements.

Table 1

Nomenclature, chemical composition, shift values determined from FTIR spectroscopy and the weight loss between 30 and 400 °C of the different samples.

| Mixtures | Si/Al molar ratio | Shift (cm ⁻¹) | Weight loss (30–400 °C) (%) |
|----------|-------------------|---------------------------|-----------------------------|
| SaMa | 1.57 | 15 | 7.8 |
| SaMaF5 | | 12 | 7.5 |
| SaMaF10 | | 8 | 7.0 |
| SaMb | 1.28 | 15 | 9.1 |
| SaMc | 1.67 | 15 | 7.9 |
| SbMa | 1.64 | 30 | 8.7 |
| SbMaF1 | | 20 | 10.3 |
| SbMaF5 | | 20 | 9.8 |
| SbMaF10 | | 20 | 9.5 |
| SbMb | 1.51 | 20 | 10.2 |
| SbMc | 1.74 | 13 | 8.9 |
| SbMcF1 | | 15 | 6.4 |
| SbMcF5 | | 15 | 6.1 |
| SbMcF10 | | 15 | 6.0 |

is used in this case) [29]. Then, the position of the band is shifted towards lower wavenumbers over time. For the first 100 min, the samples exhibit the same behavior. Then, differences can be observed depending on the metakaolin used and it is thus possible to determine the difference in the

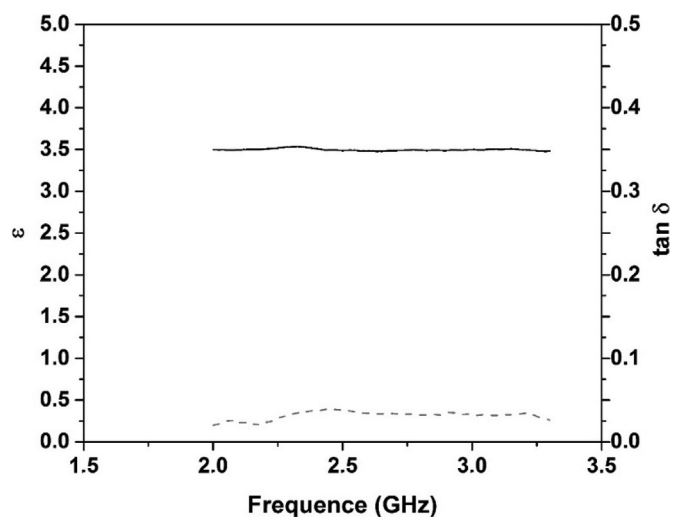


Fig. 4. Frequency dependence of permittivity and loss tangent for SaMc sample (\square ϵ ; $---$ $\tan \delta$).

Si–O–M position. The calculated shift values for all samples are reported in Table 1. For the samples without magnetite and using Sa solution, SaMb sample exhibits higher shift value than SaMa and SaMc (24, 15 and 15 cm⁻¹ for SaMb, SaMa and SaMc samples, respectively). The same variation is observed using Sb solution (30, 20 and 13 cm⁻¹ for SbMb, SbMa and SbMc samples respectively). This fact can be explained by the higher availability of reactive aluminum able to react with siliceous species from metakaolin Mb compared to Ma and Mc [30]. In fact, Mb metakaolin has a Si/Al molar ratio of 1, while Ma and Mc have higher Si/Al molar ratio (1.17 and 1.44 for Ma and Mc metakaolins, respectively). The higher Si/Al ratio reveals the presence of impurities which influence the metakaolin reactivity and is responsible for generating one or several networks. The polycondensation rate strongly depends on the reactivity of metakaolin and the alkaline solution [31]. The addition of magnetite in the SbMa mixture induces a decrease of shift value to 20 cm⁻¹ for SbMaF1, SbMaF5 and SbMaF10, respectively. The same shift value suggests that the presence of magnetite in the mixture had no influence on the formation of the species and therefore on the formation of Si–O–Al bonds. In the case of SbMc mixture, the addition of 5 or 10% of magnetite induced quite similar shift values (13, 15 and 15 cm⁻¹ for SbMc, SbMcF5 and SbMcF10). Addition of 5 and 10% of magnetite to SaMa composition induces a slight decrease of shift values (from 15 to 12

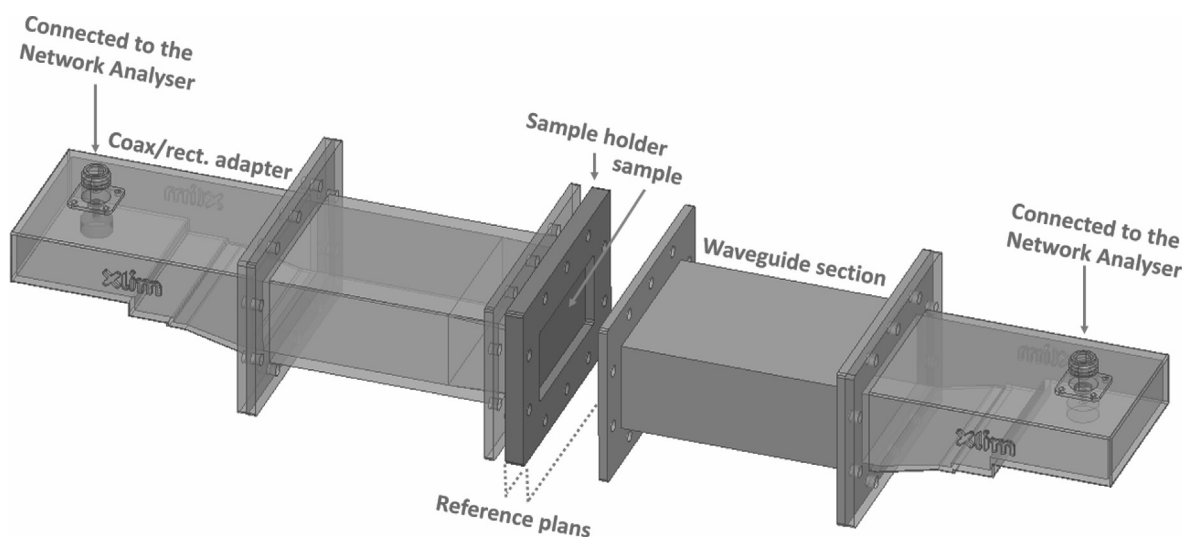
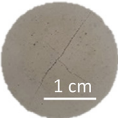
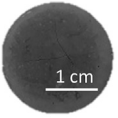


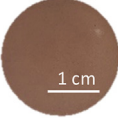
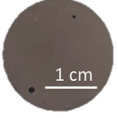
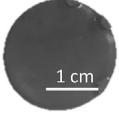



Fig. 3. Experimental setup of the loaded waveguide method in WR340 standard.

Table 2
Visual aspect of the samples with different percentage of magnetite.

| Sample | Visual aspect of samples function of Fe_3O_4 percentage (%) | | | |
|--------|---|---|---|---|
| | 0 | 1 | 5 | 10 |
| SbMa |  |  |  |  |
| SbMc |  |  |  |  |

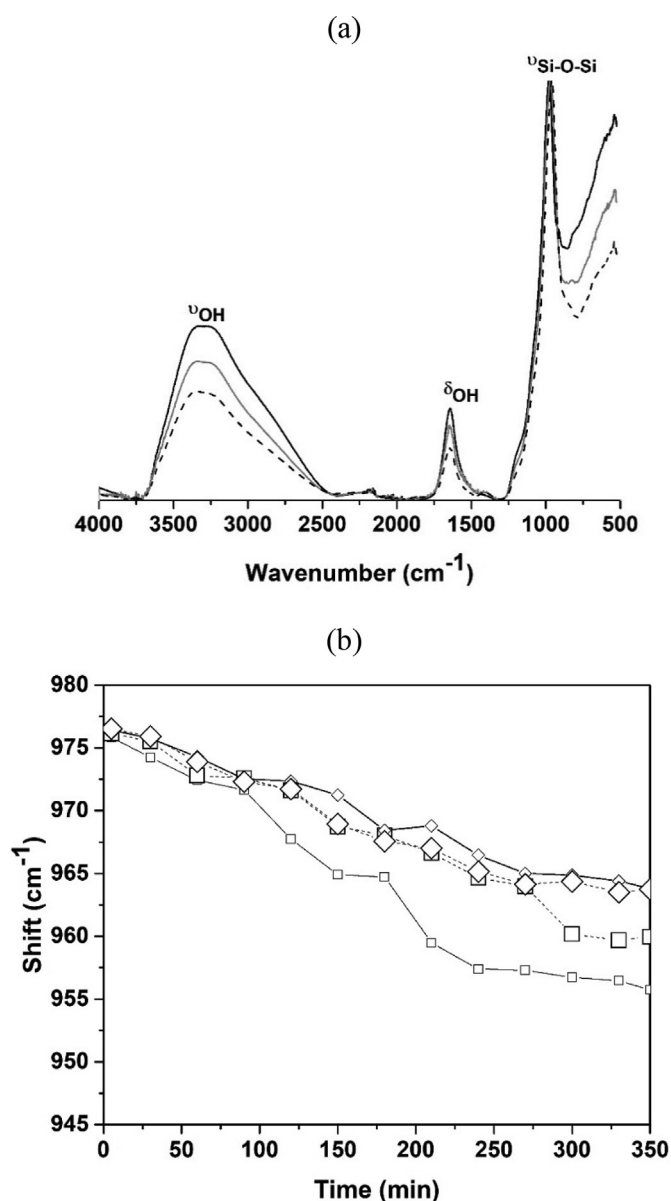


Fig. 5. (a) Example of FTIR analysis of SbMa (— $t = 0$ min; - - - $t = 360$ min; ... $t = 720$ min) and (b) Shift position versus time for different samples from FTIR spectra (\square SbMa; \square SbMaF5; \diamond SbMc; \diamond SbMcF5).

and 8 cm^{-1} for SaMa, SaMaF₅ and SaMaF₁₀ respectively). Overall results reveal that whatever the type of metakaolin, the magnetite when added with a percentage varying from 5 to 10% do not participate in the geopolymerization reaction. This finding is in agreement with literature [32] demonstrating that Fe_3O_4 , contained in the fly ash, do not participate in the reaction in fly ash based geopolymer. Other authors [33] have shown that even if the magnetite from fly ash can be dissolved, the resulting Fe did not participate in the reaction. However, the presence of magnetite modifies the reactive mixture by decreasing its surface tension (47, 38, 33, 27 mN/m for SbMa, SbMaF₁, SbMaF₅ and SbMaF₁₀ respectively). This can be explained by the low zeta potential value of magnetite which has been proven to be negative at alkali pH value [34,35].

3.2.2. Thermal analysis

Thermal analyses were performed on dried samples at 90°C . Fig. 6A shows an example of DTA-TGA curves performed on SbMa sample. Two weight losses can be distinguished corresponding to endothermic phenomena. The first weight loss between 30 and 200°C (I) represents the release of free and adsorbed water. However, the second weight loss after 200°C (II) represents the release of structural water [36]. The different weight losses for all samples are detailed in Table 1. Using Sa solution, SaMa and SaMc exhibit quite similar weight loss (8%) and lower than SaMb (9%). The same tendency is obtained with Sb solution with slightly higher weight loss values (9, 10 and 9% for SbMa, SbMb and SbMc, respectively). This finding is in accordance with the shift values showing a more favored polycondensation reaction using Sb solution and Mb metakaolin.

In order to assess the impact of magnetite on the water content, Fig. 6 B shows the evolution of the weight loss related to the release of free and physisorbed water (between $25\text{--}200^\circ\text{C}$, Fig. 6. B.a) and the total weight loss (between 25 and 800°C , Fig. 6. B.b) as a function of the percentage of Fe_3O_4 for SbMa and SbMc samples kept in air and kept in humidity for 3 days (HR 85%, 20°C). The results concerning samples kept in humidity will be discussed later. For the samples without magnetite, SbMa sample shows higher total weight loss than SbMc (11 and 9% for SbMa and SbMc samples respectively). Adding from 1 to 10% of magnetite leads to a slight decrease of the total weight loss (around 7, 10 and 6% for SaMaF_x, SbMaF_x and SbMcF_x samples respectively). Similarly, no significant change is observed concerning the weight loss related to free and physisorbed water (Fig. 6. B.a). The weight losses are quite similar around 3% for all samples. Thus, magnetite seems to have no significant effect on the water content of the sample.

To conclude, the addition of magnetite until 10 wt % in different geopolymer formulations was proven to have no or only small effect on the polycondensation reaction.

3.3. Dielectric and magnetic properties

Dielectric measurements were carried out on the different studied samples. The values of ϵ and $\tan \delta$ were investigated at room temperature

in the frequency domain between 2 and 3.3 GHz as shown in Fig. 4. As the values are quite constant in this frequency domain, the dielectric properties at 2.45 GHz were chosen to compare the different samples. The frequency range was selected since it is used for wireless communications.

a) Data for different samples

The obtained values of permittivity (ϵ) and permeability (μ) at 2.45 GHz ($T = 20\text{ }^\circ\text{C}$, 60% HR) for the different studied samples are reported in Table 3. Without magnetite addition, using Sa solution, quite similar ϵ values are obtained for the different metakaolins (3.6 ± 0.034 , 3.2 ± 0.034 and 3.5 ± 0.056 for SaMa, SaMb and SaMc samples, respectively). However, the use of Sb solution leads to higher ϵ values whatever the type of metakaolin (4.3 ± 0.11 , 4.4 ± 0.036 , 4.5 ± 0.065 for SbMa, SbMb and SbMc samples, respectively). The addition of magnetite in the case of SbMa and SbMc samples leads to a slight increase of the ϵ values (from 4.5 ± 0.025 and 4.7 ± 0.015 for 5% of magnetite addition to 4.9 ± 0.054 and 4.8 ± 0.035 when the magnetite increases to 10%). By increasing the magnetite content, the permittivity ϵ has a tendency to increase. This

indicates the content of magnetite improve the dielectric properties and storage capability of the absorber. Same behavior was observed for polymer composite doped with Fe_3O_4 [37].

Concerning the permeability (μ), without magnetite addition, Sa solution induces similar permeability values close to 1 for different metakaolins (1.01, 1.06 and 1.02 for SaMa, SaMb and SaMc samples, respectively). The use of Sb solution induces similar values (1.03, 1.05 and 1.04 for SbMa, SbMb and SbMc samples, respectively). These values are in accordance with the values of permeability found in literature for geopolymer composites [38]. The addition of magnetite induced a slight increase of permeability values due to the magnetic properties of magnetite. In SbMa samples, the increase of magnetite percentage leads to the increase of the permeability values (1.06 and 1.1 for SbMaF₅ and SbMaF₁₀ respectively). This is not the case for SbMc samples (1.03 and 1.05 for SbMcF₅ and SbMcF₁₀ respectively). Variations in permeability are close to the measurement uncertainties (few percent); it is difficult to quantify clearly the evolution of μ with the percentage of magnetite for last case.

Consequently, the magnetite addition until 10 wt % induces a slight increase of permittivity and permeability values.

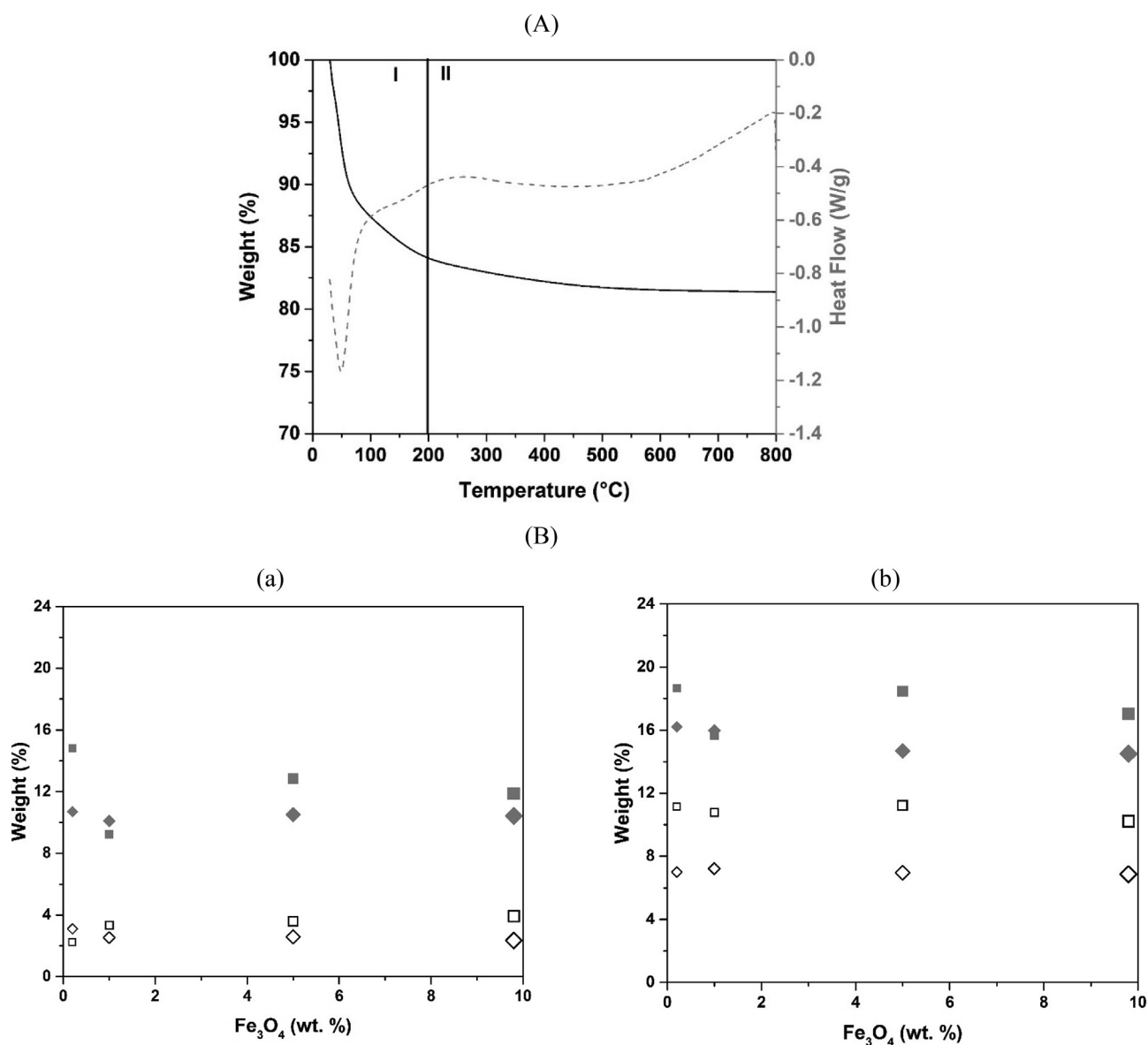


Fig. 6. (A) Example of thermogravimetric analysis and (B) weight loss values between (a) 25–200 °C (physisorbed water) and (b) 25–800 °C (total water) for samples kept at 20 °C–60% HR (\square SbMaF_x, \diamond SbMcF_x) and 20 °C–85% HR during 3 days (\blacksquare SbMaF_x, \blacklozenge SbMcF_x).

Table 3Values of ϵ , $\tan \delta$ and μ for the various samples at 2.45 GHz, 20 °C and 60% humidity after drying, 5 and 10 days.

| Sample | | | Permittivity (ϵ) at 2.45 GHz | | | Loss tangent ($\tan \delta$) at 2.45 GHz | | | Permeability (μ) at 2.45 GHz |
|------------------|--------------------|--|---|--------------|---------------|--|--------------|---------------|------------------------------------|
| Type of solution | Type of metakaolin | Percentage of Fe ₃ O ₄ | after drying | after 5 days | after 10 days | after drying | after 5 days | after 10 days | |
| Sa | Ma | 0 | 3.62 | | | 0.073 | | | 1.01 |
| | | 5 | | | | | | | |
| | | 10 | | | | | | | |
| Sb | Ma | 0 | 3.24 | 4.31 | 4.26 | 0.047 | 0.124 | 0.135 | 1.06 |
| | | 5 | | | | | | | |
| | | 10 | | | | | | | |
| Sb | Ma | 0 | 4.35 | | | 0.062 | | | 1.03 |
| | | 5 | | | | | | | |
| | | 10 | | | | | | | |
| | Mb | 0 | 4.42 | 5.77 | 5.87 | 0.082 | 0.106 | 0.128 | 1.07 |
| | | 5 | | | | | | | |
| | | 10 | | | | | | | |
| Mc | 0 | 4.46 | | | 0.090 | | | 1.10 | |
| | 5 | | | | | | | | |
| | 10 | | | | | | | | |

3.3.1. Effect of humidity and time

The impact of relative humidity was studied. The evolution of the weight loss related to the free and physisorbed water between 25 and 200 °C was plotted as a function of the percentage of Fe₃O₄ in Fig. 6B a. The weight losses after humidity exposure are at least 3 times higher than those before humidity exposure. Indeed, the weight loss between 25 and 200 °C (Fig. 6B a) increases to 14.8, 9.1, 12.9 and 11.8 for SbMa, SbMaF1, SbMaF5 and SbMaF10 respectively. The same trend is observed for SbMc samples (10.9, 10.1, 10.5 and 9.6 for SbMc, SbMcF1, SbMcF5 and SbMcF10 respectively). Consequently, the increase of water content after humidity exposure can be explained by the increase of free and physisorbed water. This type of water favors the mobility of free K⁺ and increases the electrical conductivity of the geopolymer [10,39]. This fact suggests a modification of the dielectric properties under relative humidity change. Fig. 6B b shows the evolution of the total weight (between 25 and 800 °C) deduced from thermal analysis as a function of the percentage of Fe₃O₄ for SbMa and SbMc samples kept in humidity for 3 days (HR 85%, 20 °C). Whatever the sample, an increase of the weight loss is noticed compared to those kept in air (HR 60%, 20 °C). SbMa and SbMc samples exhibit total weight losses of 19% and 16% respectively. After addition of magnetite, the total weight losses are about 16, 19 and 18% for SbMaF1, SbMaF5 and SbMaF10. For SbMc samples, the weight losses are about 16, 15 and 14% for SbMcF1, SbMcF5 and ScMaF10 respectively. Consequently, an increase of water content is evidenced for all samples with or without magnetite at high relative humidity.

In order to assess the effect of humidity and time on the dielectric properties, the samples were kept in laboratory conditions (constant temperature T = 20 °C but HR around 60%) and the dielectric properties were measured repeatedly. Fig. 7a shows the values of ϵ and $\tan \delta$ at 2.45 GHz as a function of time for SbMc samples. SbMc sample presented after 1 day a value of ϵ and $\tan \delta$ around 4.6 and 0.060 respectively. After 8 days the values of ϵ and $\tan \delta$ increase to 5.9 and 0.13, respectively). Therefore, one may conclude that the values of ϵ are stable in controlled conditions; however, the samples may evolve in time. This result leads to the hypothesis that the relative humidity fluctuation can affect the dielectric properties of geopolymer materials. To investigate the impact of humidity on dielectric properties, the samples were exposed to humidity cycling in climatic chamber (as shown in Fig. 2 in the experimental part). The dielectric properties were measured after each step. Fig. 7b presents the evolution of the dielectric properties (ϵ and $\tan \delta$) in function of time for the same sample. Samples presented initial ϵ of 4.6. After the first day in controlled humidity at 50%, the ϵ values increased to 5.8 respectively and remain stable and fixed at this value all along the period of exposure (10 days). When the humidity increases to 85%, the values of ϵ increase to 9 after 1 day and further increase up to 10 and 11 after 2 and 4 days, respectively. Setting back the humidity to 50% induces a decrease of ϵ value to 6, similar to the initial value measured at this level of humidity (5.8). A reversible behavior is thus observed with

an increase of permittivity with humidity rate from 50 to 85% and then a decrease of ϵ when getting back to initial conditions. [Humidity affects the value of ϵ , the values increase with increasing humidity, but after it is returning to lower values when the humidity decreases. Similarly, $\tan \delta$ value varies from 0.156 to 0.163 at 50% of humidity during 10 days.

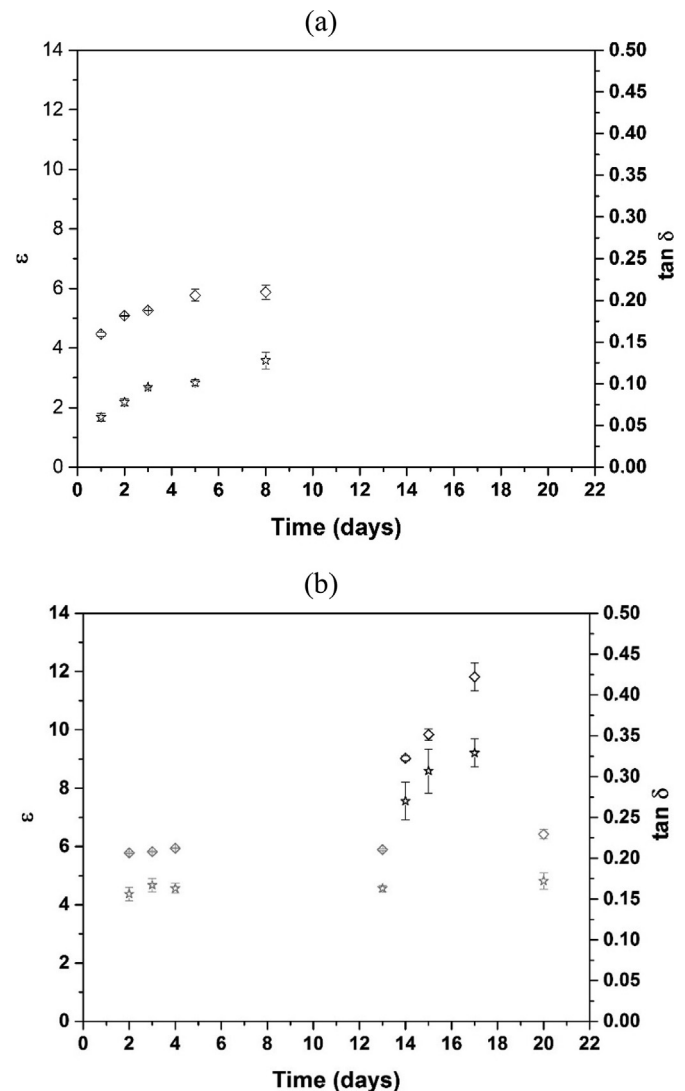


Fig. 7. Values of ϵ (\diamond) (error 0.11) and $\tan \delta$ (\star) (error 0.01) at 2.45 GHz in function of time for SbMc samples kept at 20 °C and (a) 60% humidity and (b) controlled humidity at 50% (grey) and 85% (black) by climatic chamber.

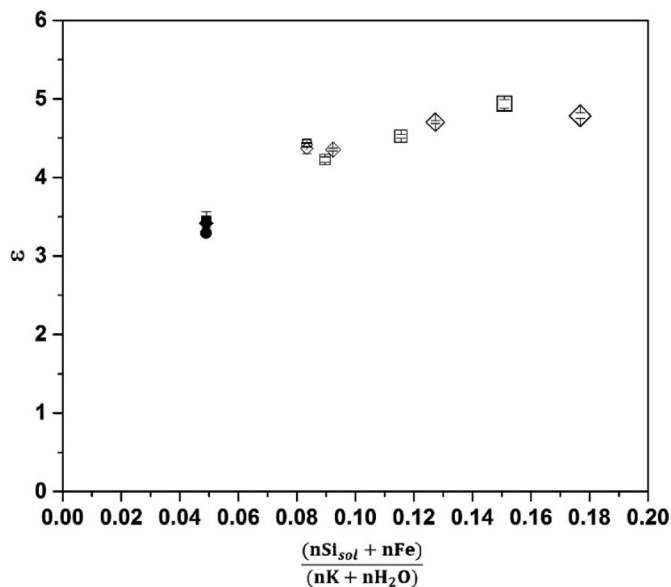


Fig. 8. Values of ϵ (error 0.05) at 2.45 GHz function of $\frac{(nSi_{sol} + nFe)}{(nK + nH_2O)}$ ratio for samples based on different solutions and metakaolin (■ SaMa; ● SaMb; ◆ SaMc; □ SbMaF_x; ○ SbMb; ◇ SbMcF_x).

Then, it increases from 0.270 to 0.329 at 85% of humidity and decreases again to 0.172 at 50% of humidity. According to literature, the dielectric loss is controlled by motion of charge-balancing cations in the alternating current field, requiring low conductivity to decrease the dielectric loss [40]. Thus, the increase of ϵ and $\tan \delta$ values upon the increase of relative humidity can be explained by the mobility of free potassium cations due to the increase of free and physisorbed water as previously demonstrated. Although this phenomenon is reversible, it is necessary to eliminate the free water in order to guaranty the stability of the dielectric properties.

3.3.2. Correlation between the dielectric properties and the chemical composition

In order to correlate the dielectric properties to the chemical composition, the variation of ϵ values at 2.45 GHz was plotted in function of $\frac{nSi_{sol} + nFe}{nK + nH_2O}$ molar ratio in Fig. 8. Only the number of moles of silicon from the activating solution was considered since the solution has an impact. A linear correlation was evidenced showing the increase of the dielectric constant ϵ as the $\frac{nSi_{sol} + nFe}{nK + nH_2O}$ molar ratio increases. Using Sa solution and without addition of magnetite, regardless of the metakaolin, the $\frac{nSi_{sol} + nFe}{nK + nH_2O}$ molar ratio is about 0.049 leading to quite similar ϵ values (3.5,

Appendices

Nicolson-Ross-Weir (NRW) [38,39] is a method to measure the electrical permittivity (ϵ) and permeability (μ) in non-conductor materials using scattering parameters (S_{ij}). This method is based on the phenomenon of reflection and transmission of a microwave electromagnetic field of the material. These phenomena occur because of the difference between the complex permittivity and the complex permeability of the two environments involved (inside and outside the material) [38,39].

Dielectric polarization takes place when the dielectric material is irradiated with an electromagnetic wave. Complex relative dielectric constant, ϵ_r , is an intrinsic property and it is not depending on the measurement method. This technique describes the interaction of microwave signals with the material. ϵ_r consists of two parts: the real part known as the dielectric constant (ϵ') which indicates the ability of the material to store microwave energy and the imaginary part known as relative loss factor (ϵ'') which indicates the dissipation of energy within the medium [41]. The relative permittivity can be calculated by following Equation (1).

$$\epsilon_r = \epsilon' - j\epsilon'' \quad (1)$$

The relationship between the real and imaginary parts is expressed as loss tangent ($\tan \delta$). The loss tangent can be used to represent the fraction of stored energy lost per period field oscillation as it is presented in equation (2).

$$\tan \delta = \epsilon'' / \epsilon' \quad (2)$$

3.2 and 3.4 for SaMa, SaMb and SaMc samples respectively). The use of Sb solution (higher nSi and lower nH₂O) leads to higher value of $\frac{nSi_{sol} + nFe}{nK + nH_2O}$ molar ratio (0.083 for SbMa, SbMb and SbMc samples respectively) and therefore increased ϵ values (4.5, 4.4 and 4.3 for SbMa, SbMb and SbMc samples respectively). The addition of magnetite in SbMa and SbMc samples increases also the $\frac{nSi_{sol} + nFe}{nK + nH_2O}$ molar ratio (from 0.090 to 0.151 and from 0.083 to for SbMaF₁, SbMaF₁₀ and SbMcF₁, SbMcF₁₀ samples respectively) leading to ϵ values varying from 4.2 to 4.9 and from 4.354 to 4.8 for SbMaF₁, SbMaF₁₀ and SbMcF₁, SbMcF₁₀ samples respectively).

Consequently, the dielectric properties are related to the chemical composition of the geopolymers. The activation solution controls the dielectric properties, magnetite shows a slight influence, while the type of metakaolin has not a significant influence.

4. Conclusion

The current study aims to develop geopolymer material for antenna applications highlighting the effect of used precursors, magnetite addition and relative humidity. For this, different formulations based on two alkaline solutions, three metakaolins containing different amounts of magnetite addition (1, 5 and 10 wt %) were synthesized. The effect of magnetite addition and the relative humidity on the polycondensation reaction, water content and dielectric properties were examined.

FTIR analysis demonstrated that magnetite until 10 wt % modified the reactive mixture but did not participate to the polycondensation reaction. Furthermore, thermogravimetric analysis reveals that the water content of the samples is influenced by the alkaline solution and the magnetite addition. Dielectric and magnetic investigations for samples without magnetite addition reveal an influence of alkaline solution type, while the type of metakaolin has a small influence. The addition of magnetite induced a slight increase of permittivity values. Concerning the magnetic properties, the permeability of the samples without magnetite addition is close to 1 for all compositions, while the addition of magnetite induces a slight increase of permeability. Humidity affects the permittivity and the loss tangent, i.e. an increase is observed with increasing humidity, but the values are decreasing back when the humidity is decreased. This result was explained by the increase of free water and cation mobility in the geopolymer.

Declaration of competing interest

The authors declare that they have no known competing financial interests or personal relationships that could have appeared to influence the work reported in this paper.

Permeability is the ability to support formation of magnetic fields in a material. It is measured in H/m (Henry/m) or N/A² (Newton/Ampere²). Relative magnetic permeability μ_r is a complex property expressed in equation (3).

$$\mu_r = \mu' - j\mu'' \quad (3)$$

The real part (μ') represents the material storage capacity of magnetic field whereas imaginary part (μ'') represents losses and power dissipation. Real part can be related to inductance and imaginary part to resistance [42].

References

- Clavier, G. Coates, J. Dumanoir, Theoretical and experimental bases for the dual-water model for interpretation of shaly sands, *Soc. Pet. Eng. J.* 24 (1984) 153–168, <https://doi.org/10.2118/6859-PA>.
- IEEE Antennas and Propagation Society Std 145 (1993).
- M. Gordon, J.L. Bell, W.M. Kriven, Thermal conversion and microstructural evaluation of geopolymers or "alkali-bonded ceramics"(ABCs), 107th Annual Meeting of the American Ceramic Society, *J. Am. Ceram. Soc.* 175 (2012) 215–224, <https://doi.org/10.1002/9781118407844.ch19>.
- H. Choo, J. Song, W. Lee, C. Lee, Effects of clay fraction and pore water conductivity on electrical conductivity of sand-kaolinite mixed soils, *J. Petrol. Sci. Eng.* 147 (2016) 735–745, <https://doi.org/10.1016/j.petro.2016.10.009>.
- H. van Olphen, *An Introduction to Clay Colloid Chemistry, for Clay Technologists, Geologists, and Soil Scientists*, vol. 2, 1977.
- N.C. Lockhart, Electrical properties and the surface characteristics and structure of clays. I. Swelling clays, *J. Colloid Interface Sci.* 74 (1980) 509–519, [https://doi.org/10.1016/0021-9797\(80\)90220-9](https://doi.org/10.1016/0021-9797(80)90220-9).
- H. Nadir, A. Gharzouni, E. Martinod, N. Feix, O. Tantot, V. Bertrand, S. Rossignol, M. Lalonde, Design of UWB Antennas Integrating Geopolymer Material, *EuCAP*, 2018, <https://doi.org/10.1049/cp.2018.1129>.
- J. Davidovits, *Geopolymer Chemistry and Applications*, fourth ed., *Institute Géopolymère, Saint-Quentin*, 2015.
- F. Pacheco-Torgal, J. Labrincha, C. Leonelli, A. Palomo, P. Chindaprasit, *Handbook of Alkali-Activated Cements, Mortars and Concretes*, Elsevier, 2015.
- A.B. Malkawi, H. Al-Mattarneh, B.E. Achara, B.S. Mohammed, M.F. Nuruddin, Dielectric properties for characterization of fly ash-based geopolymer binders, *Constr Build Mater* 189 (2018) 19–32, <https://doi.org/10.1016/j.conbuildmat.2018.08.180>.
- N. Essaïdi, H. Nadir, E. Martinod, N. Feix, V. Bertrand, O. Tantot, M. Lalonde, S. Rossignol, Comparative study of dielectric properties of geopolymer matrices using different dielectric powders, *J. Eur. Ceram. Soc.* 37 (2017) 3551–3557, <https://doi.org/10.1016/j.jeurceramsoc.2017.04.036>.
- Y. Miyamoto, S. Ishihara, T. Hirano, M. Takada, N. Suzuki, Ferroelectricity of magnetite (Fe₃O₄) observed by means of magnetoelectric effect, *Solid State Commun.* 89 (1994) 51–54, [https://doi.org/10.1016/0038-1098\(94\)90416-2](https://doi.org/10.1016/0038-1098(94)90416-2).
- A.S. Teja, P.Y. Koh, Synthesis, properties, and applications of magnetic iron oxide nanoparticles, *Prog Cryst Growth Ch* 55 (2009) 22–45, <https://doi.org/10.1016/j.pcrysgrow.2008.08.003>.
- M. Jazirehpour, S.A. Seyyed Ebrahimi, Effect of aspect ratio on dielectric, magnetic, percolative and microwave absorption properties of magnetite nanoparticles, *J. Alloys Compd.* 638 (2015) 188–196, <https://doi.org/10.1016/j.jallcom.2015.03.021>.
- H. Hausner, Influence of humidity on dielectric properties of high-frequency ceramics, *J. Am. Ceram. Soc.* 27 (1944) 175–181, <https://doi.org/10.1111/j.1151-2916.1944.tb14887.x>.
- M.J. Zouaoui, B. Nait-Ali, N. Glandut, D. Smith, Effect of humidity on the dielectric constant and electrical impedance of mesoporous zirconia ceramics, *J. Eur. Ceram. Soc.* 36 (2016) 163–169, <https://doi.org/10.1016/j.jeurceramsoc.2015.09.008>.
- H. Zhao, R.K.Y. Li, Effect of water absorption on the mechanical and dielectric properties of nano-alumina filled epoxy nanocomposites, *Compos Part A-Appl S* 39 (2008) 602–611, <https://doi.org/10.1016/j.compositesa.2007.07.006>.
- P.A.M. Steeman, F.H.J. Maurer, M.A. van Es, Dielectric monitoring of water absorption in glass-bead-filled high-density polyethylene, *Polymer* 32 (1991) 523–530, [https://doi.org/10.1016/0032-3861\(91\)90460-Z](https://doi.org/10.1016/0032-3861(91)90460-Z).
- X.M. Cui, L.P. Liu, Y. He, J.Y. Chen, J. Zhou, A novel aluminosilicate geopolymer materials with low dielectric loss, *Mater. Chem. Phys.* 130 (2011) 1–4, <https://doi.org/10.1016/j.matchemphys.2011.06.039>.
- A. Gharzouni, I. Sobrados, E. Joussein, S. Baklouti, S. Rossignol, Control of polycondensation reaction generated from different metakaolins and alkaline solutions, *J. Ceram Sci Technol* 8 (2017) 365–376, <https://doi.org/10.4416/JCST2017-00040>.
- A.M. Nicolson, G.F. Ross, Measurement of the intrinsic properties of materials by time domain techniques, *IEEE Trans. Instrum. Meas.* 19 (1970) 377–382, <https://doi.org/10.1109/TIM.1970.4313932>.
- W.B. Weir, Automatic measurement of complex dielectric constant and permeability at microwave frequencies, *Proc. IEEE* 62 (1974) 33–36, <https://doi.org/10.1109/PROC.1974.9382>.
- D. Lemaire, D. Cros, H. Jallageas, P. Guillon, Material characterisation from -160/ spl deg/C up to 800/ spl deg/C in centimeter and millimeter wavelength frequency band, *IEEE CPEM Conf. Dig.* (1996) 72–73, <https://doi.org/10.1109/CPEM.1996.546621>.
- A. Gharzouni, E. Joussein, B. Samet, S. Baklouti, S. Rossignol, Effect of the reactivity of alkaline solution and metakaolin on geopolymer formation, *J. Non-Cryst. Solids* 410 (2015) 127–134, <https://doi.org/10.1016/j.jnoncrsol.2014.12.021>.
- L. Blaney, Magnetite (Fe₃O₄): Properties, Synthesis, and Applications, 2007, p. 15, 5, <https://preserve.lehigh.edu/cas-lehighreview-vol-15/5>.
- F. Zibouche, H. Kerdjoudj, J.-B. de Lacaillerie, H. Van Damme, Geopolymers from Algerian metakaolin: influence of secondary minerals, *Appl. Clay Sci.* 43 (2009) 453–458, <https://doi.org/10.1016/j.clay.2008.11.001>.
- A. Gharzouni, E. Joussein, B. Samet, S. Baklouti, S. Pronier, I. Sobrados, J. Sanz, S. Rossignol, The effect of an activation solution with siliceous species on the chemical reactivity and mechanical properties of geopolymers, *J. Sol. Gel Sci. Technol.* 73 (2015) 250–259, <https://doi.org/10.1007/s10971-014-3524-0>.
- E. Prud'homme, A. Auteuf, N. Essaïdi, P. Michaud, B. Samet, E. Joussein, S. Rossignol, Defining existence domains in geopolymers through their physicochemical properties, *Appl. Clay Sci.* 73 (2013) 26–34, <https://doi.org/10.1016/j.clay.2012.10.013>.
- C.A. Rees, J.L. Provis, G.C. Lukey, J.S.J. van Deventer, In situ ATR-FTIR study of the early stages of fly ash geopolymer gel formation, *Langmuir* 23 (2007) 9076–9082, <https://doi.org/10.1021/la701185g>.
- A. Gharzouni, L. Vidal, N. Essaïdi, E. Joussein, S. Rossignol, Recycling of geopolymer waste: influence on geopolymer formation and mechanical properties, *Mater. Des.* 94 (2016) 221–229, <https://doi.org/10.1016/j.matdes.2016.01.043>.
- A. Gharzouni, I. Sobrados, E. Joussein, S. Baklouti, S. Rossignol, Predictive tools to control the structure and the properties of metakaolin based geopolymer materials, *Colloids Surf., A* 511 (2016) 212–221, <https://doi.org/10.1016/j.colsurfa.2016.09.089>.
- H.C. Yong, L.Y. Ming, M.M. Al Bakri Abdullah, H. Kamarudin, Thermal resistance variations of fly ash geopolymers: foaming responses, *Sci. Rep.* 7 (2017) 45355, <https://doi.org/10.1038/srep45355>.
- S.M. Nyale, O.O. Babajide, G.D. Birch, N. Böke, L.F. Petrik, Synthesis and characterization of coal fly ash-based foamed geopolymer, *Procedia Environ. Sci.* 18 (2013) 722–730, <https://doi.org/10.1016/j.proenv.2013.04.098>.
- M. Erdemoğlu, M. Sarıkaya, Effects of heavy metals and oxalate on the zeta potential of magnetite, *J. Colloid Interface Sci.* 300 (2006) 795–804, <https://doi.org/10.1016/j.jcis.2006.04.004>.
- M. Amoult, *Elaboration de mousses géopolymères à architecture poreuse contrôlée : application bâtiment*, PhD thesis, university of Limoges, 2018.
- D.S. Perera, E.R. Vance, K.S. Finnie, M.G. Blackford, J.V. Hanna, D.J. Cassidy, C.L. Nicholson, Disposition of water in metakaolin-based geopolymers, *Ceram. Trans.* 185 (2005) 225–236, <https://doi.org/10.1002/9781118407844.ch20>.
- T. Yang, R.N.C. Brown, L.C. Kempel, P. Kofinas, Magneto-dielectric properties of polymer-Fe₃O₄ nanocomposites, *J. Magn. Magn Mater.* 320 (2008) 2714–2720, <https://doi.org/10.1016/j.jmmm.2008.06.008>.
- Y. Zhang, P. He, J. Yuan, C. Yang, D. Jia, Y. Zhou, Effects of graphite on the mechanical and microwave absorption properties of geopolymer based composites, *Ceram. Int.* 43 (2017) 2325–2332, <https://doi.org/10.1016/j.ceramint.2016.11.017>.
- X.M. Cui, G.J. Zheng, Y.C. Han, F. Su, J. Zhou, A study on electrical conductivity of chemosynthetic Al₂O₃-2SiO₂ geopolymer materials, *J. Power Sources* 184 (2008) 652–656, <https://doi.org/10.1016/j.jpowsour.2008.03.021>.
- K.J.D. MacKenzie, *Innovative Applications of Inorganic Polymers (Geopolymers), Handbook of Alkali-Activated Cements, Mortars and Concretes*, Woodhead Publishing, Oxford, 2015, pp. 777–805.
- A.N. Vicente, G.M. Dip, C. Junqueira, The step by step development of NRW method, SBMO/IEEE MTT-S International Microwave and Optoelectronics Conference, 2011, pp. 738–742, <https://doi.org/10.1109/IMOC.2011.6169318>.
- X. Meng, Y. Liu, G. Han, W. Yang, Y. Yu, Three-dimensional (Fe₃O₄/ZnO)@C Double-core@shell porous nanocomposites with enhanced broadband microwave absorption, *Carbon N. Y.* 162 (2020) 356–364, <https://doi.org/10.1016/j.carbon.2020.02.035>.